# Time-Resolved Thermal Lensing Studies on Metastable Species

Chung-Chih Cheng[a] ( 鄭仲志 ), Guo-Ray Wu[b]* ( 吳國瑞 ), Chau-Shuen Chiou[c] ( 邱朝順 ), Jen-Kan Yu[d] ( 余人侃 ) and Pi-Tai Chou[d]* ( 周必泰 )

[a]*Department of Chemistry, Fu-Jen Catholic University, Shin Chuang 242, Taiwan, R.O.C.*

[b]*Toko University, Pu-Tzu City, Chia-Yi County 603, Taiwan, R.O.C.*

[c]*Department of Chemistry, National Chung-Cheng University, Chia-Yi 621, Taiwan, R.O.C.*

[d]*Department of Chemistry, National Taiwan University, Taipei 106, Taiwan, R.O.C.*

Time-resolved thermal lensing (TRTL) techniques have been applied to resolve photophysical and thermodynamic parameters for various metastable species, of which the relaxation dynamics are dominated by the radiationless transition. Using 1H-phenalen-1-one as a sensitizer, the lifetime ($\tau_\Delta$), absolute quantum yield ($\Phi_\Delta$) and efficiency of generation ($S_\Delta^T$) of singlet molecular oxygen ($^1\Delta_g$) have been determined in various organic solvents. In particular, through the development of an ultrasensitive detecting system, TRTL studies on the relaxation dynamics of $O_2(^1\Delta_g)$ become feasible in aqueous solution. In another application, based on the TRTL technique in combination with the $O_2$ sensitization experiment, the $T_1$-$S_0$ energy gap of the proton-transfer tautomer in 3-hydroxyflavone, which is otherwise inaccessible due to the dominant radiationless deactivation, has been deduced to be ~ 8500 ± 1020 $cm^{-1}$.

**Keywords:** Time-resolved thermal lensing; Singlet molecular oxygen; Excited-state intramolecular proton transfer.

## INTRODUCTION

The time-resolved thermal lensing (TRTL) method has been recognized as a powerful technique for detecting the heat released through nonradiative processes of the excited molecules.[1] Its high sensitivity has allowed one to measure ultraweak absorption spectra,[2] prototypes among which are two-photon spectroscopy,[3] vibrational overtone spectroscopy[4] and analyses of nonemissive transient species at low concentrations.[5-8] Since the thermal lensing measurement is essentially a calorimetric determination of a very small temperature gradient induced by relaxation of excited species, it further provides direct information on the enthalpy change during photophysical and/or photochemical reactions.[9] Recently, two-color laser excitation TRTL techniques have been successfully applied to probe the reaction energetics and dynamics of the excited transient species.[7,10]

In this study, we report the application of the TRTL technique to resolving the dynamics as well as energetics of several crucial metastable species, among which singlet molecular oxygen and triplet states of excited-state intramolecular proton transfer molecules will receive particular attention. The photophysics of the $^1O_2$, ($^1\Delta_g$) species has been extensively investigated due to its important role in photochemical and biological processes.[11-14] However, the detection of $O_2$ $^1\Delta_g \rightarrow {}^3\Sigma_g^-$ phosphorescence in the solution phase is nontrivial due to its dominant radiationless deactivation and near infrared ~ 1273 nm $^1\Delta_g \rightarrow {}^3\Sigma_g^-$ (0,0) transition, which is beyond the spectral response of normal photomultiplier tubes. An alternative way to detect $^1O_2$ may rely on the observation of its nonradiative transition to the ground state.[9,15-17] The TRTL method is superior to conventional ones in that the absolute yield of transient species can be extracted from the experiment without the requirement of an additional standard reference.[18] Consequently, the corresponding photophysical parameters can be extracted directly. In this study, through the application of an ultrasensitive detecting system, the temporal response of TRTL can be as fast as the transient acoustic time so that studies of relaxation dynamics of $O_2(^1\Delta_g)$ in $H_2O$ become feasible. In another approach, many molecules exhibiting the excited-state intramolecular proton transfer (ESIPT) reaction, energetics and dynamics of the tautomer triplet state ($T_1$', hereafter the prime sign denotes the proton-transfer tautomer species) are rarely found. The correlation of a forbidden triplet → singlet radiative decay rate constant, $k_P$, generally obeys the relationship of $k_P \propto |D|^2\bar{\nu}^3$ where $D$ is the transition moment length and $\bar{\nu}$ is the average wavenumber of the transition.[19] $k_P$ is then proportional to $E_T^3$,

Dedicated to Professor Fa-Ching Chen on the occasion of his ninetieth birthday.

where $E_T$ denotes the energy gap between $T_1$' and $S_0$' states, and becomes smaller when $E_T$ decreases to the near infrared (NIR) region. Furthermore, a theory pertaining to the radiationless decay concludes that the intramolecular radiationless deactivation should increase upon decreasing the energy gap of the transition.[20] Particularly, for many ESIPT molecules vibrational modes associated with intramolecular hydrogen bonds usually act as a good quencher for the tautomer emission.[21] Thus, detecting phosphorescence in the NIR region, especially for the ESIPT molecules, may be hampered by the dominant $T_1' \rightarrow S_0'$ radiationless deactivation process. In this study, we will apply 3-hydroxyflavone, a well-known ESIPT molecule, as a prototype to demonstrate the potential of the TRTL technique in resolving photophysical properties of the tautomer triplet states.

## EXPERIMENTAL SECTION

### Materials

1H-phenalen-1-one (PH, Aldrich) was purified by column chromatography (n-hexane:ethyl acetate 1:1 v/v) followed by recrystallization twice in methanol. 3-Hydroxyflavone (3HF, Aldrich, 99.0%) and 5-Hydroxyflavone (5HF, Lancast, 98.0%) were twice recrystallized in ethanol. Solvents were of spectrograde quality and used without further purification. $O_2$-saturated solutions were used in the sensitization experiment. Conversely, measurements of triplet-state relaxation dynamics were performed under $O_2$ free conditions, in which the solution was degassed through three freeze-pump-thaw cycles.

### Measurements

The setup of TRTL measurements in this study is depicted in Fig. 1. A 3rd harmonic of the Nd:YAG laser (355 nm) was used as a pump pulse, of which the output energy could be fine-tuned through a combination of λ/2 plate and Glan-Thomson polarizer. A He-Ne laser (JDS Uniphase 1125; 632.8 nm, 5 mW) equipped with a stabilized power supply was used as an analyzing beam for TRTL signals. The He-Ne beam was focused in front of the sample cell with an f = 30 mm lens, and was in a direction of 180° with respect to the Nd:YAG excitation beam (focused by an f = 200 mm lens). The He-Ne laser beam after the sample cell was passed through a pinhole (Corion 2401; 300 μm diameter) and an appropriate combination of filters. The beam intensity was then detected with a red sensitive, fast response photomultiplier (Hamamatsu model R5509-72) operated at -80 °C. Typically, an average of 512 shots were acquired for each measurement. To determine the acoustic transient time, the output impedance of the photomultiplier was reduced to 50 Ω, giving a system response limited by the duration of a laser pulse of ~ 6 ns. However, for most applications, an output impedance of 1K Ω was applied in order to increase the TRTL S/N ratio. In this case the system response time was increased to ~ 120 ns (vide infra).

Steady state and time-resolved measurements of near-IR $O_2(^1\Delta_g \rightarrow {}^3\Sigma_g^-$ (0,0)) phosphorescence have been elaborated in our previous reports.[22] Briefly, the steady state emission was obtained by exciting the sample solution under a front-face excitation configuration using an Ar ion laser (362 nm, Coherent Innova 90). The emission was then sent through a near-IR Fourier-transform interferometer (Bruker Equinox 55) and detected by a slow response (rise time ~ 5 ms), highly sensitive liquid nitrogen cooled Ge detector (403, Applied Detector Corporation). For the time-resolved study, the sample was exited by a 3rd harmonic (355 nm) of the Nd:YAG laser, of which the emission was collected and sent through a fast response (rise time ~ 0.3 μs) Ge detector (403HS, Applied Detector Corporation). The decay profile was monitored by a 2.5 GHz bandwidth transient digitizer (Lecroy 9360).

Steady-state UV-Vis absorption and fluorescence spectra were recorded with a Hitachi (U-3310) spectrophotometer and an Edinburgh (FS 920) fluorimeter, respectively.

## RESULTS AND DISCUSSION

### Optimization of the TRTL measurements

The optimization of the system based on temporal re-

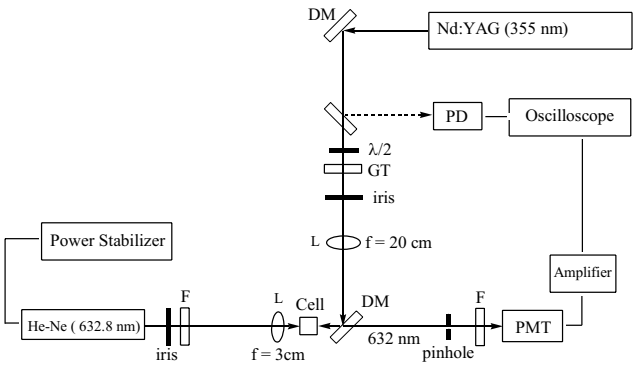


Fig. 1. A schematic diagram of the current TRTL setup: F, filter; L, lens; DM, dichroic mirror; GT, Glan-Thompson polarizer; PD, photodiode; PMT, photomultiplier tube.

Table 1. Properties of Various Solvents at 298 K[a]

| Solvent | $D$ ($\times 10^{-7}$, $m^2s^{-1}$) | κ ($\times 10^{-2}$, cal $cm^{-1}s^{-1}$ $^oC$) | ($d\eta/dT$) ($\times -10^{-4}$, $K^{-1}$) | $w_p$ (μm) | $v_a$ ($\times 10^3$, $ms^{-1}$) | $t_c$ (ms) | $\tau_a$ (ns) |
|---|---|---|---|---|---|---|---|
| $H_2O$ | 1.36 | 0.58 | 0.9 | 54 | 1.48 | 5.3 | 36.0 |
| MeOH | 1.00 | 0.20 | 3.9 | 40 | 1.00 | 4.0 | 40.0 |
| EtOH | 0.90 | 0.18 | 3.7 | 40 | 1.01 | 4.3 | 39.6 |
| Cyclohexane | 0.83 | 0.12 | 5.3 | 53 | 1.28 | 8.5 | 41.4 |
| Benzene | 1.06 | 0.16 | 5.6-6.4 | 49 | 1.25 | 5.5 | 39.2 |
| Acetonitrile | 1.70 | 0.17 | 4.6 | 55 | 1.30 | 4.4 | 42.3 |

$D$, the thermal diffusivity; κ, the thermal conductivity; ($d\eta/dT$), the temperature coefficient of the refractive index; $w_p$, beam radius of excitation laser; $v_a$, sound velocity; $t_c$, thermal time constant; $\tau_a$, acoustic transient time.
[a] see Ref. 23.

sponse and laser power dependence plays a key role in successful TRTL measurements. The intrinsic response of the current setup was first determined by the temporal resolution of light scattering from the output of a Ti-Sapphire laser (730 nm, 150 fs), and was estimated to be ~ 2 ns from its full width at half maximum (fwhm) of the temporal profile. The system response, however, should be further limited by the duration of ~ 6 ns of the pump pulse (3rd harmonic of the Nd:YAG laser) used in the TRTL study. Nevertheless, the actual temporal limitation of the TRTL signal mainly depends on the acoustic transient time defined as

$$\tau_a = w_p/v_s \quad (1)$$

where $w_p$ is the radius of the pump-beam waist at the focal point, which was measured to be ~ 50 μm in our current setup (vide infra), $v_s$ denotes the speed of sound in the solvent, and is in the range of $1.0 \times 10^3 \sim 1.48 \times 10^3$ m/s among various solvents studied.[23] Applying eq. (1), an acoustic transient time was calculated to be < 50 ns in all studied solvents (see Table 1). This derivation could further be tested experimentally by the TRTL study of 5-hydroxyflavone (5HF). Photophysical properties of 5HF have been well established. In cyclohexane, 5HF undergoes a barrierless ESIPT (< 100 fs), followed by an ultrafast decay of the proton-transfer tautomer fluorescence ($\tau_f$ = 1.2 ps, $\Phi_f \sim 10^{-5}$).[24] The rate constant of the ground-state reverse proton transfer was also estimated to be >> $10^{12}$ $s^{-1}$ so that an overall proton-transfer cycle (i.e. the recovery process) in 5HF takes place within a period of a few picoseconds. This, in combination with ~ unity radiationless deactivation, makes 5HF an ideal model to monitor the acoustic transient time for our current TRTL configuration. As shown in Fig. 2, upon the 355-nm excitation in cyclohexane 5HF revealed a fast but finite rise in the TRTL signal. Its assignment to the transient acoustic kinetics can be further ascertained by the observation of an oscillating TRTL signal resulting from a round trip of the acoustic wave. Taking the temporal full width at half maximum (fwhm) of the peak, the acoustic transient time was estimated to be a ~ 50 ns in cyclohexane, which within experimental error, is consistent with the theoretical derivation of ~ 40 ns.

It is worth noting that the output impedance of the photomultiplier was reduced to 50 Ω for the above measurement (see experimental section). However, in the following studied systems the life spans of the transient species examined are normally > 1 μs. To increase the S/N ratio of TRTL signals we instead used an output impedance of 1K Ω. In this case the system response time has been increased to ~ 120 ns, and the acoustic wave could no longer be resolved.

In order to insure the TRTL signals are free from interferences of multiphoton excitation and/or saturation effects, the system was further optimized by using the benzophenone/

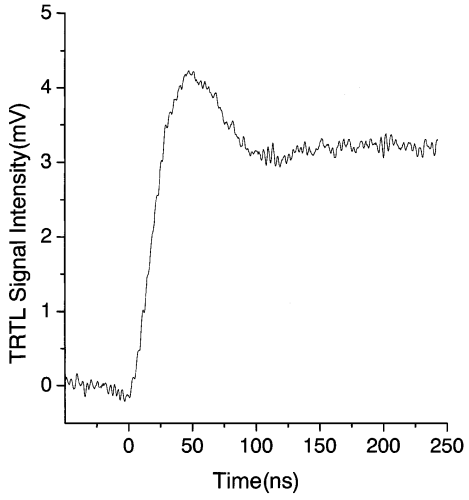


Fig. 2. The TRTL signal of 5HF ($5.2 \times 10^{-5}$ M) in cyclohexane with an acoustic-wave oscillation shown at the initial portion of the rise component.

benzene solution. As shown in Fig. 3, a typical TRTL signal of benzophenone in benzene ($\lambda_{ex}$ ~ 355 nm) was composed of fast and slow rise components, followed by a much longer decay profile of ~ 1.2 ms (not shown here) attributed to the thermal diffusion. The fast component ($U_F$), which correlates well with the acoustic transient time after the laser irradiation, is ascribed to the heat released through nonradiative deactivation processes from the initially prepared excited singlet state to either the ground or triplet state. Conversely, the slow rise component ($U_S$) originates from the triplet benzophenone relaxing to the ground state. Within a range of e.g. < 100 μs, in which the contribution of thermal diffusion can be neglected, the experimental results can be well fitted by two exponential components expressed as

$$f(t) = b_0 + U_F e^{-k_F t} + U_S e^{-k_S t} \tag{2}$$

where $k_F$ ($U_F$) and $k_S$ ($U_S$) denote the rate constant (amplitude) of fast and slow components, respectively, and $b_0$ is an offset parameter. The best nonlinear least-squares fit of *f(t)* gave the faster component, $k_F$, to be within the range of $1.0 \times 10^7$ $s^{-1}$, which is consistent with the system response of ~ $8.3 \times 10^6$ $s^{-1}$. In fact, upon fixing $k_1$ by $8.3 \times 10^6$ $s^{-1}$ and only varying $U_F$, $U_S$ and $k_S$, the results are nearly the same as those obtained by relaxing all parameters. Accordingly, $k_S$ was deduced to be ~ $1.67 \times 10^5$ $s^{-1}$ ($\tau_S$ ~ 6.0 μs), consistent with the lifetime of the triplet benzophenone of 5.5 μs reported in the literature.[6] Laser power dependent TRTL experiments have also been performed by monitoring the total amplitude of the initial thermal lens signal $U_T$ (= $U_F$ + $U_S$) as a function of the pump laser energy. As shown in the insert of Fig. 3, good linear relations were maintained when the laser energy was kept as low as 40 μJ/pulse, indicating a one-photon process for the observed TRTL signals. Hereafter, typical excitation energies of < 40 μJ were applied throughout the remaining studies.

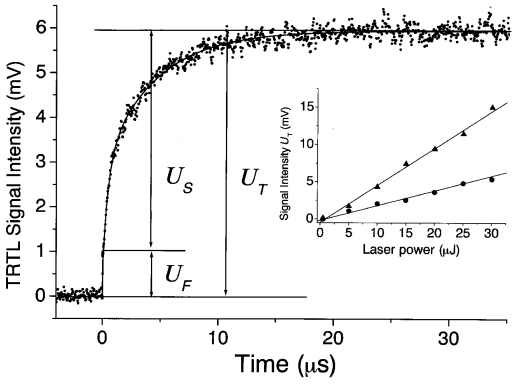


Fig. 3. The TRTL profile of benzophenone ($1.0 \times 10^{-4}$ M) in degassed benzene with 355 nm excitation, and its laser power dependences of the total heat, $U_T$, at different concentrations. The solid lines are best-fitting curves obtained with the least-squares method.($k_F$: $8.3 \times 10^6$ $s^{-1}$, $k_S$: $1.67 \times 10^5$ $s^{-1}$, $U_F$: -0.00105, $U_S$: -0.00489, see eq. (2)). The relation between lens signal and laser power maintained is sufficiently linear in the depicted ranges. The absorbance at 355 nm was prepared to be 0.2 (•) and 0.5 (▲).

For the case of benzophenone, the ratio for *Us* versus $U_T$ can theoretically be expressed as

$$\frac{U_S}{U_T} = \frac{\Phi_{isc} E_T}{h\nu_{ex} - \Phi_f E_f} \tag{3}$$

where $\Phi_{isc}$ denotes the yield of $S_1 \rightarrow T_1$ intersystem crossing, $h\nu_{ex}$ and $E_T$ are energies of the excitation light (337 kJ/mol) and the triplet state for benzophenone (287 kJ/mol),[23] respectively. $E_f$ is the averaged fluorescence energy, and $\Phi_f$ denotes the yield of fluorescence, which is essentially ~ 0 in benzene at 298 K. Accordingly, $\Phi_f F_f$ is negligibly small and can thus be neglected in eq. (3). Plugging $U_S/U_T$ of 0.84 in this study, $\Phi_{isc}$ was determined to be 0.99 ± 0.01, which, within experimental error, is identical with the ~ unity value reported previously,[23] supporting the optimization of the current TRTL system.

**Photophysical parameters of $O_2$ ($^1\Delta_g$)**

On the basis of a fully optimized TRTL system, i.e. ~ 120 ns temporal resolution and one-photon excitation, our first approach is to study photophysical parameters of $O_2$ ($^1\Delta_g$) in the solution phase. The associated photophysical and photochemical pathways upon exciting suitable sensitizers in the presence of $O_2$ are depicted in Scheme I.

**Scheme I**

$$S_0 \xrightarrow{h\nu} S_1 \tag{4}$$

$$S_1 \xrightarrow{k_f} S_0 + h\nu_f \tag{5}$$

$$S_1 \xrightarrow{k_{ic}} S_0 \tag{6}$$

$$S_1 \xrightarrow{k_{isc}} T_1 \tag{7}$$

$$T_1 + {}^3O_2 \rightarrow S_0 + {}^3O_2 \tag{8}$$

$$T_1 \rightarrow S_0 \tag{9}$$

$$T_1 + {}^3O_2 \xrightarrow{k_{et}} S_0 + {}^1O_2 \tag{10}$$

$${}^1O_2 \xrightarrow{k_d} {}^3O_2 \tag{11}$$

As shown in Scheme I, a fraction of the energy absorbed initially by a sensitizer may be released through pro-

cesses (4)-(10) within the system response time of < 120 ns in an aerated or oxygenated solution. The nonradiative processes (6)-(10) are all responsible for the fast heat generation ($U_F$) observed in the TRTL experiment. In the absence of $^1O_2$ acceptors, the rest of the absorbed energy, which is redistributed as the excitation energy of $^1O_2$, is degraded to heat through process (11) with a much slower rate and thus contributes to the slow, resolvable component (i.e. $U_S$) in the TRTL signal.

Using 1H-phenalen-1-one (PH) as a sensitizer, a typical TRTL signal in, e.g., $O_2$-saturated benzene is shown in Fig. 4a. Applying the best curve fitting based on eq. (2) a $k_S$ value of $3.32 \times 10^4$ s$^{-1}$ ($\tau_S \sim 30$ μs) was then deduced. In comparison, the time-resolved $O_2$ $^1\Delta_g \rightarrow {}^3\Sigma_g^-$ (0,0) 1273 nm phosphorescence was also studied using the same sample (Fig. 4b), and the decay time was fitted to be ~ 31 μs. The consistency between TRTL and phosphorescence in relaxation dynamics further ascertains the *Us* component to be resulting from the $O_2$ $^1\Delta_g \rightarrow {}^3\Sigma_g^-$ (0,0) radiationless deactivation. Similar correlations between TRTL and phosphorescence on the $O_2(^1\Delta_g)$ relaxation dynamic were also observed in other organic solvents, and the results are listed in Table 2.

With the fast response capability and ultrahigh sensitivity, an attempt has also been made to resolve the TRTL signal associated with relaxation dynamics of $O_2$ ($^1\Delta_g$) in $H_2O$. The main difficulty of this approach is the intrinsically weak lensing signal in $H_2O$. Theoretically, the TRTL signal, $S(t)$, is expressed as

$$S(t) \sim 16lzN\alpha \int_0^t H(t-\tau)(1+2\tau/t_c)^{-2} d\tau \qquad (12)$$

where $H(t)$ is the heat function,[9] $l$ and $z$ denote the thickness of the thermal lens and the distance from the focal point of the converging lens to the sample, respectively, and $t_c$ is the thermal time constant.[25] According to eq. (12) it is apparent that $S(t)$ is proportional to α, which can be further expressed as $\frac{D(d\eta/dT)}{\kappa J w_p^4}$, where $D$ denotes the thermal diffusivity (cm$^2$s$^{-1}$), κ is the thermal conductivity (cal cm$^{-1}$s$^{-1}$ °C), $J = 4.18$ J cal$^{-1}$, and $(d\eta/dT)$ is the temperature coefficient of the refractive index. These parameters are solvent dependent and their values are listed in Table 1. Plugging all relevant parameters, the value of α and hence the TRTL signal in $H_2O$ was estimated to be ~ 20 times less than that in, e.g., benzene under the same experimental conditions. This, in combination with its fast relaxation dynamics (vide infra), makes the TRTL approach to $O_2(^1\Delta_g)$ in $H_2O$ rather difficult. Nonetheless, as shown in the insert of Fig. 4a, the TRTL for $O_2(^1\Delta_g)$ was obtained for the first time in the $O_2$-saturated $H_2O$. On the basis of eq. (2), the decay was then fitted to be ~ 2.3 μs, which is on the same magnitude as those reported based on the $^1\Delta_g \rightarrow {}^3\Sigma_g^-$ (0,0) emission (see Table 2).[26-28]

We further applied eq. (3) to determine the absolute yields, $\Phi_\Delta$, of $O_2(^1\Delta_g)$ production. Note in eq. (3) $\Phi_{isc}$ is simply replaced by $\Phi_\Delta$ in the sensitization experiment. For example, the ratio for $U_S$ versus $U_T$ was measured to be 0.25 in MeOH. Conversely, $hv_{ex}$ and $E_T$ are energies of the excitation

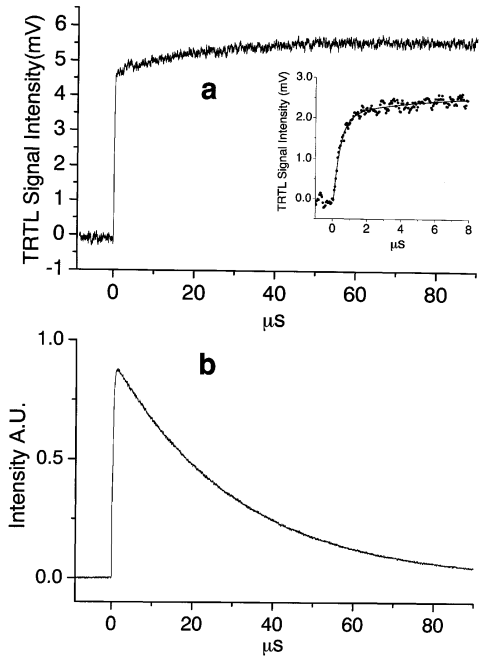


Fig. 4. **a.** The TRTL profile and **b**. the decay dynamics of the $O_2$ $^1\Delta_g \rightarrow {}^3\Sigma_g^-$ (0,0) 1273 nm emission of $O_2$ ($^1\Delta_g$) sensitized by PH ($6.5 \times 10^{-5}$ M) in $O_2$-saturated benzene. Insert: the TRTL profile of $O_2$ ($^1\Delta_g$) in $H_2O$. ($k_F$: $8.3 \times 10^6$ s$^{-1}$, $k_S$: $4.35 \times 10^5$ s$^{-1}$, $U_F$: -0.00238, $U_S$: -0.00018).

Table 2. Absolute Quantum Yields $\Phi_\Delta$ and Lifetime $\tau_\Delta$ of $^1O_2$ Sensitized by PH in Several $O_2$-Saturated Solvents

| Solvent | $\tau_\Delta$ (μs) [a] | $\tau_\Delta$ (μs) [b] | $\Phi_\Delta$ | $\Phi_\Delta$ [c] |
|---|---|---|---|---|
| $H_2O$ | 2.3 | 4.2 | 0.90 | 0.98 |
| MeOH | 8.5 | 10.4 | 0.91 | 0.98 |
| EtOH | 13 | 15.3 | 0.90 | - |
| Cyclohexane | 22 | 23.0 | 0.89 | 0.98 |
| Benzene | 30 | 31.2 | 0.95 | 1.00 |
| Acetonitrile | 60 | 58.3 | 0.92 | 1.00 |

[a] Data obtained from TRTL measurements in this study.
[b] Data obtained from the luminescence studies, see Ref. 26.
[c] see Ref. 29.

($\lambda_{ex}$: 355 nm, 28,169 $cm^{-1}$) and $O_2(^1\Delta_g \rightarrow {}^3\Sigma_g^-(0,0))$ transition (~ 7,855 $cm^{-1}$), respectively. Furthermore, it is also reasonable to assume a negligible $\Phi_f F_f$ value in the case of benzophenone due to its lack of fluorescence in the solution phase at 298 K. As a result, $\Phi_\Delta$ was determined to be 0.91 ± 0.01 in MeOH. This value, within experimental error, is comparable with the reported value of 0.98 via the luminescence/photoacoustic approach.[29] $\Phi_\Delta$ values in other organic solvents are listed on Table 2, which are all in good agreement with the reported value of near unity (see Table 2 for comparison). Note $\Phi_\Delta$ in water obtained in the TRTL experiment is also located in the category of ~ 0.90.

Nevertheless, as indicated in Table 2, the lifetimes measured with TRTL tend to be shorter than those from luminescence experiments. Similarly, the quantum yields determined with TRTL are smaller than those determined with other measurements by 5-9%. Such a discrepancy is believed to result from the differences in the power of excitation between the two methods. The (laser) power-dependent decay as well as emission efficiency of $^1O_2$ emission has been reported in numerous sensitization experiments.[28] Although the mechanisms associated vary case by case, it has been widely accepted that quenching of $^1O_2$ by radicals generated from the photodissociation of sensitizers/solvents might play a key role. Since the excitation laser beam has to be focused, a more prominent quenching effect should take place in the TRTL study in comparison to the luminescent method in that a defocused, low power laser beam was applied. At this stage, because types of radicals generated from sensitizer PH or solvents are still unknown, and are not the main focus in this study, there is no further detailed discussion regarding quenching mechanisms.

Theoretically, absolute quantum yields of the $O_2(^1\Delta_g)$ production, $\Phi_\Delta$, can be expressed as $\Phi_\Delta = \Phi_{isc} P_{O_2}^T S_\Delta^T$ (13) and $P_{O_2}^T = \dfrac{k_q[O_2]}{k_T^0 + k_q[O_2]}$ (14) where $P_{O_2}^T$ is defined as the fraction of the triplet PH quenched by $O_2$, $k_q$ is the bimolecular quenching constant of $O_2$ and $k_T^0$ is the decay rate constant of the triplet PH excluding the $O_2$ quenching process. $S_\Delta^T$ denotes the efficiency of the $O_2(^1\Delta_g)$ generation, which is the fraction of the triplet state quenched by oxygen that yields $O_2(^1\Delta_g)$. As shown in process (8) of Scheme I, it is possible that not every collision of triplet PH with oxygen will generate $^1O_2$. Thus, $S_\Delta^T$ deserves carefully examination in order to determine the efficiency of singlet oxygen generation. $P_{O_2}^T$ expressed in eq. (14) is valid only if a long-lived triplet sensitizer as well as low triplet concentrations are prepared, ensuring negligible triplet-triplet annihilation and ground state self-quenching.[30]

According to the theory of electron-exchange type of energy transfer, the overall spin must be conserved upon forming a collisional complex. Since the sum of spin vector in the $T_1$-$O_2$ complex gives a combination of quintet, triplet and singlet, the possibility of each collision generating $^1O_2$ is 1/9. This viewpoint holds true in most $O_2$ sensitization reactions. It is thus adequate to adopt a $k_q$ value directly from 1/9 of the diffusion controlled rate derived from the Stokes-Einstein equation,[31] which is, e.g., $3.2 \times 10^9$ $M^{-1}s^{-1}$ in cyclohexane. Giving the oxygen saturated concentration of ~ $1.15 \times 10^{-2}$ M in cyclohexane,[32] a value of $3.68 \times 10^7$ $s^{-1}$ for $k_q[O_2]$ was then deduced, which is apparently >> $k_T^0$. It is thus reasonable to assume $P_{O_2}^T$ to be near unity in cyclohexane. Similar results of ~ unity $P_{O_2}^T$ value were also concluded in other studied solvents. Knowing $\Phi_{isc}$ of PH to be nearly solvent independent and equivalent to ~ 100%,[27] it is reasonable to conclude that $S_\Delta^T$ is nearly identical with $\Phi_\Delta$ in the PH sensitizing $^1O_2$ experiments, which is > 0.9 in various solvents studied. Among aromatic compounds investigated as singlet oxygen sensitizers, Redmond and Braslavsky[15] have shown a qualitative difference between n,π* and π,π* types of sensitizers, with the latter having higher $S_\Delta^T$ values (0.9 ± 0.1) than the former (0.30 ± 0.05). Our results of $S_\Delta^T \geq 0.90$ in the TRTL study, in combination with a π,π* character[29] of the triplet PH, are consistent with Redmond and Braslavsky's proposal.

**Probing triplet state energetics/dynamics for the ESIPT molecules**

In another approach we have applied 3HF to demonstrate the potential of the TRTL technique in deducing the dynamics and energetics of the tautomer triplet state. Upon $S_0 \rightarrow S_1$ (π,π*, $\lambda_{max}$ ~ 355 nm) excitation, 3HF undergoes an ultrafast rate of ESIPT, resulting in a 526-nm tautomer fluorescence with $\Phi_f$ as high as ~ 0.36 ± 0.02 (in cyclohexane, see Scheme II).[33] Based on an ideal 4-level electronic system, 3HF has been demonstrated as the first case to exhibit prominent lasing action.[33] Due to its anomalously large Stokes shift and high yield of tautomer fluorescence, 3HF and its analogues have been used in numerous applications.[34-36] Unfortunately, further practical applications are limited by its photooxygenation originating from the tautomer triplet state,[37] of which the population is appreciable based on the transient absorption studies.[38,39] The corresponding $T_1$'-$S_0$' gap for the tautomer species, which is of key importance for probing the reaction energetics, remains unknown due to the lack of the tautomer phosphorescence spectrum. The main obstacle is due to the dominant radiationless transition in the $T_1$' state even at a temperature as low as 10 K.[40] In addition, the weak 5-membering intramolecular hydrogen bond is sub-

**Scheme II** Structures of 3-hydroxyflavone in normal and tautomer forms, and the associated ESIPT reaction

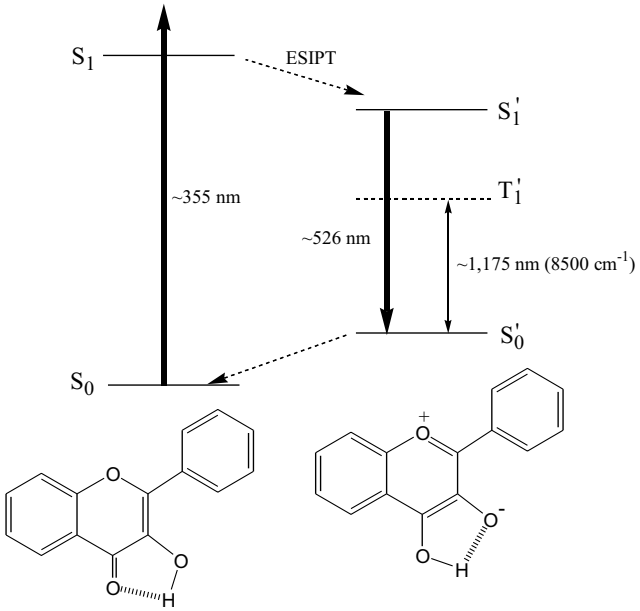


ject to protic solvent perturbation as well as self-aggregation at low temperatures, prohibiting the ESIPT reaction.[41,42]

Fig. 5 reveals the TRTL signal of 3HF in degassed cyclohexane, in which a slow $U_S$ component was apparently resolvable. On the basis of eq. (2), the slow decay component was best fitted to be 5.8 μs, which is on the same magnitude as ~ 7-10 μs reported previously using the transient absorption technique.[38,39] Because $U_S$ is rather small, the uncertainty of $U_S/U_T$ becomes significant. In this study, using an average of 5 experiments the $U_S/U_T$ was calculated to be 0.05 ± 0.006 in the degassed solution. Due to the broad tautomer fluorescence, $E_f$ was calculated from its average value expressed as $< E_f > = \frac{\int I_f(\tilde{\nu})\tilde{\nu}d\tilde{\nu}}{\int I_f(\tilde{\nu})d\tilde{\nu}}$ where $I_f(\tilde{\nu})$ denotes the relative emission intensity as a function of wavenumber. Accordingly, a value of 18,255 $cm^{-1}$ was obtained.

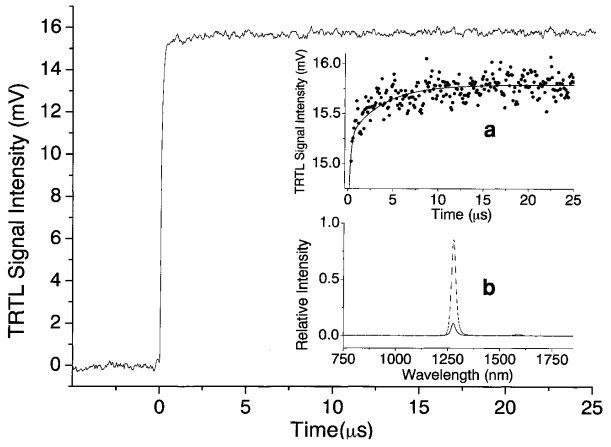


Fig. 5. The TRTL signal of 3HF ($2.2 \times 10^{-5}$ M) in degassed cyclohexane. The absorbance was prepared to be ~ 0.3 at the excitation wavelength of 355 nm. Insert: (a) the appearance of $U_S$ signal at 15-16 mV, ($k_F$: $8.3 \times 10^6$ $s^{-1}$, $k_S$: $1.72 \times 10^5$ $s^{-1}$, $b_0$: 0.0158, $U_F$: -0.015, $U_S$: -0.000789). (b) The $O_2$ $^1\Delta_g \rightarrow {}^3\Sigma_g^-$ (0,0) 1273 nm emission spectrum in cyclohexane sensitized by (-----) PH or (—) 3HF under the same optical density of 0.3 at 362 nm ($Ar^+$ laser).

However, $E_T$, i.e. the $T_1$'-$S_0$' gap, cannot be extracted from eq. (3) without knowing the value of $\Phi_{isc}$. On the basis of an indirect triplet(3HF)/triplet(naphthalene) energy transfer experiment, $\Phi_{isc}$ of 3HF has been deduced to be ~ 0.18.[39] Limited by the donor/acceptor overlap efficiency and precision of the triplet-triplet transient absorption, this method may be subject to appreciable uncertainties. Alternatively, we performed an oxygen photosensitization experiment in order to circumvent this obstacle. This method becomes feasible for determining the yield of the triplet state of organic molecules if the following assumptions hold: (i) The $T_1$-$S_0$ energy gap is greater than the energy required to sensitize singlet oxygen ($O_2$ $^1\Delta_g \rightarrow {}^3\Sigma_g^-$ (0,0) of ~ 7855 $cm^{-1}$). (ii) Sensitization of oxygen by the $S_1$ state is negligible due to its relatively much shorter life span. (iii) The decay of the triplet state should be dominated by the $T_1$-$^3O_2$ energy transfer. (ii) holds true for the case of 3HF due to the fast decay of the tautomer fluorescence at room temperature (~ 3.2 ns in cyclohexane at 298 K). Furthermore, based on the transient absorption study, an ~ 1/9 diffusion controlled $O_2$ quenching rate has been reported in 3HF.[39] Thus, under the oxygen saturated condition ($1.15 \times 10^{-2}$ M in cyclohexane at 1 atmosphere $O_2$, 298 K) the decay of the triplet state should be dominated (> 99%) by the $T_1$'-$^3O_2$ energy transfer, fulfilling the requirement (iii).

The insert of Fig. 5(b) shows the emission spectrum of $O_2$ $^1\Delta_g \rightarrow {}^3\Sigma_g^-$ (0,0) transition at 1273 nm sensitized by 3HF, of which the lifetime was determined to be ~ 21 μs in methylcyclohexane. Within experimental error, the decay dynamics are identical to those of the $O_2$ ($^1\Delta_g$) emission in cyclohexane sensitized by PH.[29] We have further determined the triplet-state population in 3HF by comparing its sensitized $O_2$ ($^1\Delta_g$) emission intensity with respect to that produced with the sensitizer PH. The ratio of the sensitized $O_2$ ($^1\Delta_g$) emission intensity for 3HF versus PH was deduced to be 0.13 in

the $O_2$ saturated methylcyclohexane. Counting the PH sensitized $O_2$ ($^1\Delta_g$) yield of 0.98 ± 0.1[29] and ~ unity of the triplet state quenching dynamics for 3HF in the $O_2$ saturated cyclohexane (vide supra), the yield of intersystem crossing, $\Phi_{isc}$ was then estimated to be 0.127. In this derivation, we have assumed that the production of $O_2(^1\Delta_g)$ sensitized by the triplet state is of unit efficiency. This assumption is based on a spin statistical argument that the only deactivation pathway of the triplet state resulting from the $T_1$'-$O_2$ ($^3\Sigma_g^-$) encounter is the energy transfer to form $O_2$ ($^1\Delta_g$). Since the assumption of unit efficiency of $O_2$ ($^1\Delta_g$) generation in each $T_1$'-$^3O_2$ encounter may be invalid for the case of 3HF, we put the value of $\Phi_{isc}$ = 0.127 as a lower limit. Plugging all parameters deduced into eq. (3), the $T_1$'-$S_0$' gap was then estimated to be 8500 ± 1020 $cm^{-1}$, which is consistent with a value of ~ 8000 $cm^{-1}$ predicted from the semi-empirical approaches.[43] The deduced $T_1$'-$S_0$' energy gap is nearly isoenergetic with respect to the $O_2(^1\Delta_g \rightarrow {}^3\Sigma_g^-$ (0,0)) transition, supporting the assumption (i) and the high efficiency of 3HF in sensitizing $^1O_2$, followed by the oxygenation (i.e. insertion) reactions.[37]

## CONCLUSION

In conclusion, we have demonstrated TRTL to be a powerful and reliable technique in detecting the dynamics and energetics of the metastable species. In one approach, the relaxation dynamics, absolute $\Phi_\Delta$ and $S_\Delta^T$ values of $O_2$ ($^1\Delta_g$) have been determined by TRTL in various solvents, particularly in $H_2O$ where the extremely weak TRTL signal with corresponding fast decay dynamics have been resolved. In another approach, the $T_1$'-$S_0$' gap of ~ 8500 $cm^{-1}$ in 3HF has been deduced, which is otherwise spectroscopically inaccessible through the luminescent methods. It is thus proposed that similar approaches can be applied to other ESIPT molecules lacking spectral and dynamic information on the triplet states. Future approaches of the TRTL technique aimed at probing dynamics and energetics of short-lived metastable species are feasible. For example, through the luminescence/photoacoustic studies, it has been concluded that in the PH sensitizing $O_2$ experiment $O_2(^1\Sigma_g^+)$ and $O_2(^1\Delta_g)$ were produced in yields of 0.62 and 0.93, respectively, in $CCl_4$.[29] The decay time of $O_2(^1\Sigma_g^+)$ has been reported to be as short as ~ 130 ns in $CCl_4$,[29,44] which is mainly dominated by the $^1\Sigma_g^+ \rightarrow {}^1\Delta_g$ radiationless deactivation. From both energetics and symmetry points of view, $O_2(^1\Sigma_g^+)$ species may be more reactive as well as undergo different types of reaction pathways with respect to those of the $^1\Delta_g$ state. It is thus intriguing to resolve the TRTL signal attributed to the $^1\Sigma_g^+$ state and subsequently monitor its reaction dynamics. Focus on this is currently in progress.

## ACKNOWLEDGEMENT

Financial supports from the National Science Council, Republic of China, are gratefully acknowledged.

Received September 25, 2002.

## REFERENCES

1. For example, see: Braslavsky, S. E.; Heihoff, K. *Handbook of Organic Photochemistry*; CRC Press: Boca Raton, FL. 1988.
2. Whinnery, J. R. *Acc. Chem. Res.* **1974**, *7*, 225.
3. Twarowski, A. J.; Kliger, D. S. *Chem. Phys.* **1977**, *20,* 253.
4. Swofford, R. L.; Long, M. E.; Albrecht, A. C. *Science* **1976**, 191.
5. Dovichi, N. D.; Harris, J. M. *Anal. Chem.* **1979**, *51*, 728.
6. Suzuki, T.; Okuyama, U.; Ichimura, T. *J. Phys. Chem. A* **1997**, *101*, 7047.
7. Nagano, M.; Suzuki, T.; Ichimura, T. *Analytical Sciences* **2001**, *17*, s26.
8. Ha, J. H.; Jung, G. Y.; Kim, S. M.; Lee, Y. H.; Shin, K.; Kim, Y. R. *Bull. Korean Chem. Soc.* **2001**, *22*, 63.
9. Fuke, K.; Ueda, M.; Itoh, M. *J. Am. Chem. Soc.* **1983**, *105*, 1091.
10. Takatori, Y.; Suzuki, T.; Kajii, Y.; Shibuya, K.; Obi, K. *Chem. Phys*. **1993**, *169*, 291.
11. Chou, P. T.; Frei, H. *Chem. Phys. Lett.* **1985**, *122*, 87.
12. Chou, P. T.; Chen, Y. C.; Wei, C. Y.; Lee, M. Z. *J. Am. Chem. Soc.* **1998**, *120,* 4883.
13. Li, C.; Hoffman, M. Z. *J. Phys. Chem. A* **2000**, *104*, 5998.
14. Schmidt, R.; Shafii, F. *J. Phys. Chem. A* **2001**, *105*, 8871.
15. Redmond, R. W.; Braslavsky, S. E. *Chem. Phys. Lett.* **1988**, *148*, 523.
16. Bossbroich, C.; Garcia, N. A.; Braslavsky, S. E. *J. Photochem.* **1985**, *31*, 37.
17. Heihoff, K.; Redmond, R. W.; Braslavsky, S. E.; Rougee, M.; Salet, C.; Faver, A.; Bensasson, R. V. *Photochem. Photobiol.* **1990**, *51*, 635.
18. Terazima, M.; Tonooka, M.; Azumi, T. *Photochem. Photobiol*. **1991**, *54*, 59.
19. McGlynn, S. P.; Azumi, T.; Kinoshita, M. *Molecular Spectroscopy of the Triplet State*; Prentice Hall Englewood Cliffs, N. J. 1969, p 18.
20. Sieband, W. *J. Chem. Phys*. **1967**, *47*, 2411.
21. For example, see: Klöpffer, W. *Adv. Photochem.* **1977**, *10*,

311.
22. Chou, P. T.; Wu, G. R.; Liu, Y. I.; Yu, W. S.; Chiou, C. S. *J. Phys. Chem. A* **2002**, *106*, 5967.
23. Murov, S. L.; Carmichael, I.; Hug, G. L. *Handbook of Photochemistry*, 2nd ed.; Marcel Dekker: New York, 1993.
24. Chou, P. T.; Chen, Y. C.; Yu, W. S.; Cheng, Y. M. *Chem. Phys. Lett.* **2001**, *340*, 89.
25. where $D$ denotes the thermal diffusivity, $t_c$ correlates with the observed millisecond thermal diffusion in TRTL measurements, and can be used to estimate the beam waist $w_p$, see: Friedrich, D. M.; Klem, S. A. *Chem. Phys.* **1979**, *41*, 153.
26. Rodgers, M. A. J. *J. Am. Chem. Soc.* **1983**, *105*, 6201.
27. Chou, P. T.; Khan, S.; Frei, H. *Chem. Phys. Lett.* **1986**, *129*, 463.
28. Wessels, J. M.; Rodgers, M. A. J. *J. Phys. Chem.* **1995**, *99*, 15725, *and references therein.*
29. (a) Schmidt, R. *Ber. Bunsen-Ges. Phys. Chem*. **1992**, *96*, 794. (b) Schmidt, R.; Bodesheim, M. *Chem. Phys. Lett*. **1993**, *213*, 111. (c) Schmidt, R.; Tanielian, C.; Dunsbach, R.; Wolff, C. *J. Photochem. Photobiol. A* **1994**, *79*, 11.
30. Abdel-Shafi, A. A.; Beer, P. D.; Mortimer, R. J.; Wilkinson, F. *J. Phys. Chem. A* **2000**, *104*, 192.
31. For example, see: Birks, J. B. *Photophysics of Aromatic Molecules*; Wiley: New York, 1970, p 313.
32. Battino, R.; Rettich, T. R.; Tominaga, T. *J. Phys. Chem. Ref. Data* **1983**, *12(2)*, 163.
33. Chou, P. T.; McMorrow, D.; Aartsma, T. J.; Kasha, M. *J. Phys. Chem*. **1984**, *88*, 4596.
34. Renschler, C. L.; Harrah, L. A. *Nucl. Inst. Methods Phys. Rev.* A235, Sept., U. S. Patent, **1985**, 635.
35. Sytnik, A.; Kasha, M. *Proc. Natl. Acad. Sci.* **1994**, *91*, 8627.
36. Roshal, A. D.; Grigorovich, A. V.; Doroshenko, A. O.; Pivovarenko, V. G. *J. Phys. Chem. A* **1998**, *102*, 5907.
37. Studer, S. L.; Brewer, W. E.; Martinez, M. L. *J. Am. Chem. Soc.* **1989**, *111*, 7643.
38. Itoh, M.; Fujiwara, Y.; Sumitani, M.; Yoshihara, K. *J. Phys. Chem.* **1986**, *90*, 5672.
39. Brewer, W. E.; Studer, S. L.; Standiford, M.; Chou, P. T. *J. Phys. Chem.* **1989**, *93*, 6088.
40. Brewer, W. E.; Studer, S. L.; Chou, P. T. *Chem. Phys. Lett.* **1989**, *158*, 345.
41. McMorrow, D.; Kasha, M. *J. Phys. Chem.* **1984**, *88*, 2235.
42. McMorrow, D.; Kasha, M. *Proc. Natl. Acad. Sci. U.S.A*. **1984**, *81*, 3375.
43. Dick, B. *J. Phys. Chem.* **1990**, *94*, 5752.
44. Chou, P. T.; Wei, G. T.; Lin, C. H.; Wei, C. Y.; Chang, C. H. *J. Am. Chem. Soc.* **1996**, *118*, 3031.